


## Article

# Multisatellite Task Allocation and Orbit Planning for Asteroid Terminal Defence

Yuelong Luo, Xiuqiang Jiang \* , Suchuan Zhong, Yuandong Ji and Guohao Sun

School of Aeronautics and Astronautics, Sichuan University, Chengdu 610207, China; yuelong@stu.scu.edu.cn (Y.L.); sczhong@scu.edu.cn (S.Z.); jyd1127@scu.edu.cn (Y.J.); sgh2019@scu.edu.cn (G.S.)  
\* Correspondence: jiangxiuqiang@scu.edu.cn

**Abstract:** Near-Earth asteroids are a great threat to the Earth, especially potential rendezvous and collision asteroids. To protect the Earth from an asteroid collision, it is necessary to investigate the asteroid defence problem. An asteroid terminal defence method based on multisatellite interception was designed in this study. For an asteroid intruding in the sphere of the gravitational influence of the Earth, multiple interceptor satellites are used to apply a kinetic energy impulse to deflect the orbit of the asteroid. First, the effects of planned interception time and planned interception position on the required impulse velocity increment applied to the asteroid are assessed for interception opportunity selection. Second, multiple interceptor satellites are selected to perform the defence task from the on-orbit available interceptor satellite formation. An improved contract net protocol algorithm considering the Lambert orbital manoeuvre is designed to fulfil the task allocation and satellite orbit planning. Finally, simulation experiments demonstrate the rationale and effectiveness of the proposed method, which provides support for asteroid terminal defence technology.

**Keywords:** asteroid defence; multisatellite interception; task allocation; orbit planning



**Citation:** Luo, Y.; Jiang, X.; Zhong, S.; Ji, Y.; Sun, G. Multisatellite Task Allocation and Orbit Planning for Asteroid Terminal Defence. *Aerospace* **2022**, *9*, 364. <https://doi.org/10.3390/aerospace9070364>

Academic Editor: Fanghua Jiang

Received: 14 May 2022

Accepted: 5 July 2022

Published: 7 July 2022

**Publisher's Note:** MDPI stays neutral with regard to jurisdictional claims in published maps and institutional affiliations.



**Copyright:** © 2022 by the authors. Licensee MDPI, Basel, Switzerland. This article is an open access article distributed under the terms and conditions of the Creative Commons Attribution (CC BY) license (<https://creativecommons.org/licenses/by/4.0/>).

## 1. Introduction

In recent years, asteroids have caused harm and damage to humans. In astronomy, an asteroid with an orbital perihelion distance of 1.3 Astronomical Units (AU) or less is called a near-Earth asteroid (NEA). NEAs are faint, widely distributed, and difficult to find. Their orbit is easily altered by the traction of large planets [1]. Throughout history, asteroids have been impacting the Earth. For the estimated flux of these objects as a function of size [2]. On 30 June 1908, a huge explosion caused by an asteroid occurred near the Podkamennaya Tunguska River in Siberia, Russia, flattening some 2000 square km of forest [3]. On 15 February 2013, an asteroid with a diameter of about 20 m exploded over the Chelyabinsk region of Russia, sending many fragments to the ground, damaging a large number of buildings and injuring more than 1200 people [4,5]. The above events demonstrate that asteroid impacts are a significant potential long-term threat to humanity. Therefore, the study of asteroid defence is of great value and challenge. Researchers have conducted numerous studies in the fields of asteroid monitoring [6], orbit calculation [7–9], and asteroid landing and detection [10–14]. Additionally, space debris monitoring systems can provide information support for asteroid defence. For example, European ground-based systems for space debris monitoring [15–17] are involved in the European Space Surveillance and Tracking project [18] and collect data to perform orbit determination of all observed objects. When asteroids are close to the Earth, radar monitoring systems can provide observational information to facilitate terminal asteroid defence.

In terms of asteroid defence, existing research has focused on trajectory prediction, risk assessment, and defence approaches. Yu et al. designed indirect and direct transfer trajectories to rendezvous with NEAs and proposed two assessment methods of the accessibility of NEAs using stand-alone CubeSats [19]. There are two main categories

of in-orbit treatments for threatening asteroids. The first is a transient action approach based on kinetic impact, and the second is a long-term action approach based on laser ablation, dragging, and gravitational traction, which is still in the conceptual exploration stage. The National Aeronautics and Space Administration (NASA) and European Space Agency (ESA) have collaborated on the Asteroid Impact and Deflection Assessment (AIDA) mission to test asteroid dynamics impact techniques and asteroid deflection effects [20]. Wagner et al. investigated the target selection for a hypervelocity asteroid interceptor flight validation mission and validated the effectiveness of a Hypervelocity Asteroid Interceptor Vehicle (HAIIV) concept [21]. On this basis, Wie et al. presented a new mission concept of exploiting a multiple kinetic-energy impactor vehicle (MKIV) system that does not employ nuclear explosives to disrupt or pulverise hazardous asteroids with a short warning time [22]. Existing asteroid defence means are primarily aimed at defending against asteroids outside the Earth's gravitational capture range in the expectation of breaking the asteroid or deflecting its orbit. However, some asteroids are discovered only a short time before they impact the Earth. When these threatening asteroids are discovered, they have already invaded the sphere of the gravitational influence of the Earth and are approaching the Earth. However, for the asteroid with a short warning time and close distance, disruption is usually considered, and coordinated defence by multiple interceptor satellites is rarely considered [22].

To overcome the above deficiencies, this study focuses on terminal defence interception based on multiple interceptor satellites for an asteroid within 380,000 km from the Earth. For such NEAs, the energy required to change their orbits is too large and exceeds the capability of current non-nuclear kinetic energy interceptors. Therefore, this study first assesses the impulse velocity increment applied to the asteroid that is required to successfully intercept it. Then, a multisatellite coordinated interception approach is designed for the terminal defence of the NEA that invades the sphere of the gravitational influence of the Earth. An improved contract net protocol algorithm considering the Lambert orbital manoeuvre is proposed to implement defence task allocation and orbit planning. The main contributions of this study are as follows:

- (1) Multisatellite-based terminal defence strategy for the asteroid that invaded the sphere of the gravitational influence of the Earth is investigated. It can be regarded as a remedial measure after the failure of early defence means and as a method to defend against suddenly discovered/invading asteroids.
- (2) The effect law of interception positions on the magnitude of the required impulse velocity increment applied to the invading asteroid is disclosed. It can be a reference for defensive interception strategy formulation.
- (3) An improved contract net protocol algorithm considering the Lambert orbital manoeuvre is proposed to realise the coupling of defence task allocation and orbit planning, which can accomplish terminal asteroid defence with multisatellite cooperative interception.

The rest of this paper is organised as follows. In Section 2, the problem description and model of terminal asteroid defence are presented. In Section 3, the analysis method of asteroid interception position selection is presented, giving the magnitude of the impulse velocity increment applied to the asteroid required to complete the terminal asteroid defence and analysing the effect of the interception position and interception time on it. Section 4 proposes an improved contract net protocol algorithm considering the Lambert orbit manoeuvre, which implements the coupling of defence task allocation and orbit planning. In Section 5, numerical simulation and analysis are presented. Finally, Section 6 contains a conclusion.

## 2. Problem Description

### 2.1. Terminal Asteroid Defence Scenario Description

The problem of asteroid defence for the end phase based on multisatellite interception studied in this work can be described as follows. At the near-Earth orbit altitude, multiple interceptor satellites are distributed in a Walker constellation. When an impact-threatening

asteroid enters the gravitational capture range of the Earth, the interceptor satellites collaborate to intercept the asteroid and thus deflect the satellite orbit to keep it at a safe distance from the Earth. In this paper, asteroid defence is achieved through coordinated satellite interception.

For the interception approach, based on the idea of the directed energy (DE) system of planetary defence from [23], it was assumed that each interceptor satellite carries an asteroid impulse generator, which can apply an impulse force to the asteroid in any direction, and the impulse magnitude that the asteroid impulse generator can provide is  $I_s$ .

**Remark 1.** As stated in [23], the directed energy system is still in the proof-of-concept stage. To support the implementation of the asteroid defence mission in this paper, based on the idea of controllable energy direction, this paper assumes that the impulse generator is capable of applying an impulse force of controllable direction to the asteroid, which can be generated by a high-energy impulse rocket.

Interceptor satellites must first rendezvous with asteroids through orbital manoeuvres [24]. Then, the asteroid impulse generator applies an impulse force to the asteroid after the interceptor satellite makes rendezvous contact with the asteroid to alter the motion of the asteroid.

Therefore, the interceptor satellite transfer process is a rendezvous process with a terminal constraint of Equation (1). The rendezvous process of the interceptor satellite with the asteroid is a double-impulse manoeuvre process. The first impulse puts the interceptor satellite into the transfer orbit, and the second impulse makes the interceptor satellite satisfy the terminal constraint of Equation (1).

$$\begin{aligned} r_{a,\text{end}} - r_{s,\text{end}} &= 0 \\ v_{a,\text{end}} - v_{s,\text{end}} &= 0 \end{aligned} \quad (1)$$

where  $r_{a,\text{end}}$  is the asteroid position vector at the end of the interceptor satellite transfer,  $r_{s,\text{end}}$  is the interceptor satellite position vector at the end of the interceptor satellite transfer,  $v_{a,\text{end}}$  is the asteroid velocity vector at the end of the interceptor satellite transfer, and  $v_{s,\text{end}}$  is the interceptor satellite velocity vector at the end of the interceptor satellite transfer.

After the rendezvous, we consider the asteroid deflection process. Through space-based and ground-based observation networks, we can make observations [24], orbit predictions [25], and threat assessments [26] of the asteroid to obtain its mass and orbital elements. The relationship between the impulse magnitude and the momentum of the asteroid is shown in Equation (2):

$$I_s = m_1 v_1 - m_0 v_0 \quad (2)$$

where  $m_0$  and  $v_0$  are the mass and velocity of the asteroid before receiving the impulse action and  $m_1$  and  $v_1$  are the mass and velocity of the asteroid after receiving the impulse action.

According to related studies [27–29], the energy loss and momentum change patterns in different cases have large differences, which have a significant impact on the asteroid interception efficiency. However, since the focus of this study is on the task allocation and orbit planning of intercepting satellites, the following simplified assumptions on the asteroid interception process are made:

**Assumption 1.** The mass of the asteroid does not change during the entire interception process, and the effect of the mass of the intercepting satellite after the rendezvous is ignored.

**Assumption 2.** The action time of the asteroid impulse generator thrust is very short, and it is considered to change the asteroid motion state instantaneously.

**Assumption 3.** The impulse generated by the asteroid impulse generator will be fully transferred into the momentum of the asteroid.

Based on the above assumptions, Equation (2) can be rewritten as Equation (3), and we can solve for the impulse velocity increment that each interceptor satellite can provide:

$$I_s = m_0 \cdot \Delta v \quad (3)$$

where  $\Delta v = v_1 - v_0$  is the impulse velocity increment applied to the asteroid.

Due to the poor mission robustness and mission inefficiency of a single interceptor satellite, multiple interceptor satellites are needed to intercept an asteroid cooperatively at the same predetermined intercept position to change the flight orbit of the asteroid and keep it at a safe distance from the Earth. A schematic diagram of the cooperative asteroid-interception scene in this study is shown in Figure 1.

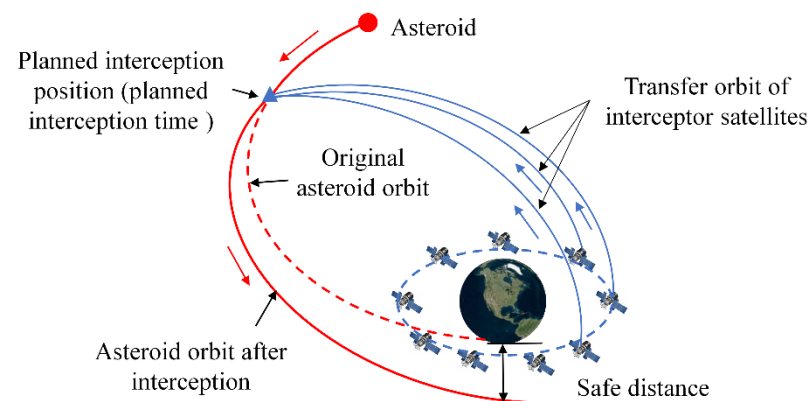


**Figure 1.** Schematic diagram of a cooperative asteroid-interception scene.

In the terminal asteroid defence scenario, the selection of the interception time has an important impact on the urgency of the defence mission, the required impact impulse size, and the energy consumption of the interceptor satellite orbital manoeuvre. In this study, first, the simulation analysis of asteroid orbits based on orbital dynamics theory was conducted to study the mechanism and rule of the interception time on the defence mission to select the suitable interception position. Then, defence task allocation was performed considering the task time constraint, manoeuvring capability constraint, and satellite transfer orbit information to select satellites from the standby interceptor satellite formations. In the existing task allocation algorithms, the task allocation was mostly separated from the orbit planning, and the satellite orbit planning was performed separately after the task allocation was completed, ignoring the influence of the actual orbit on the execution of the task, which cannot obtain the best task allocation results. To address the above shortcomings, this study adopted the contract net protocol algorithm to construct a multisatellite task allocation model, considered the influence of satellite interception orbits on the task allocation cost at the task allocation level, and obtained the transfer orbits of each interception satellite by solving the Lambert rendezvous problem. The algorithm completes orbit planning during the task allocation period and realizes the coupling of task allocation and transfer orbit planning.

The main flow of the presented method is shown in Figure 2. In this figure,  $t_i$  is the  $i$ -th planned interception time,  $t_{step}$  is the time step,  $\Delta$  denotes the impulse velocity increment applied to the asteroid in the  $j$ -th subloop,  $v_{step}$  is the velocity step,  $d_p$  is the distance of the planned interception position from the Earth,  $r_{safe}$  denotes the safe distance of asteroids from the Earth, and  $R_i$  is the revenue function corresponding to the  $i$ -th planned interception time.

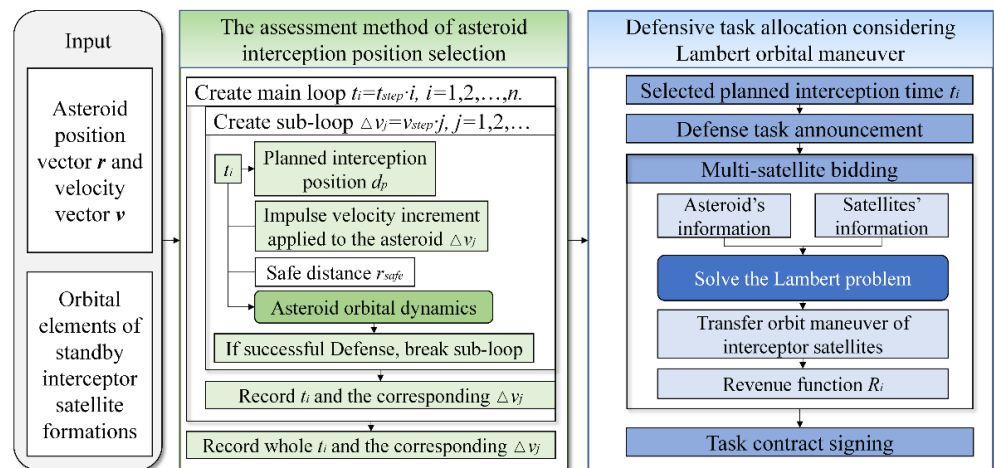


Figure 2. Flow chart of the proposed terminal asteroid defence method.

2.2. Coordinate System and Modelling

In this study, we defend against asteroids that have entered the gravitational capture range of the Earth and therefore establish the Earth-Centred Inertial (ECI) coordinate system, with the Earth as the central object [30]. The ECI coordinate system is a typical Cartesian coordinate system (CCS). Its coordinate origin is the Earth core O, the Z-axis points northwards along the axis of the Earth’s rotation, the X-axis points to the vernal equinox of the Earth, the Y-axis and the XZ plane form a right-handed coordinate system, and the XY plane is the equatorial plane. Among them, the ecliptic plane is the orbital plane of the Earth’s rotation around the Sun, and the vernal equinox is the ascending intersection of the Earth’s equatorial line and the ecliptic plane. The ECI coordinate system is shown in Figure 3.

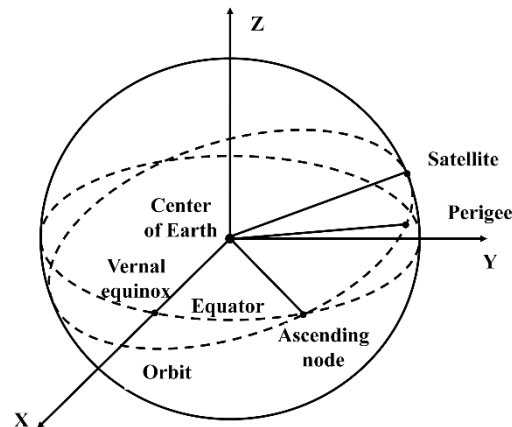


Figure 3. Schematic diagram of the ECI coordinate system.

The ECI coordinate system is geostationary and does not change with the rotation of the Earth. However, in practice, the ECI coordinate system still has a small variation due to the slow change in the Earth’s rotation axis and the weak perturbation of the ecliptic plane.

The dynamics model for the two-body problem is set as Equation (4) [31]:

$$\begin{cases} dr_x/dt = v_x \\ dr_y/dt = v_y \\ dr_z/dt = v_z \\ dv_x/dt = -\mu x/r^3 \\ dv_y/dt = -\mu y/r^3 \\ dv_z/dt = -\mu z/r^3 \end{cases} \quad (4)$$

where  $[x, y, z]^T$  and  $[v_x, v_y, v_z]^T$  are the position and velocity vectors of the asteroid or satellites,  $r = \sqrt{x^2 + y^2 + z^2}$ , and the Earth's gravitational constant is assumed to be  $\mu = 398,600 \times 10^9 \text{ m}^3/\text{s}^2$ .

The state information of asteroid and interceptor satellites is represented by position vectors and velocity vectors, as shown in Equation (5):

$$\begin{cases} \text{Asteroid} = \{r_a, v_a\} \\ \text{Satellite} = \{r_s, v_s\} \end{cases} \quad (5)$$

For satellites in the elliptical orbit, the state information can also be expressed in terms of the orbital elements as Equation (6):

$$\text{Satellite} = \{a, ecc, inc, raan, argp, nu\} \quad (6)$$

where  $a$  denotes the semi-major axis of the orbital plane,  $ecc$  denotes the eccentricity,  $inc$  denotes the orbital inclination,  $raan$  denotes the right ascension of the ascending node,  $argp$  denotes the argument of perigee, and  $nu$  denotes the true anomaly.

### 3. Asteroid Interception Position Assessment and Selection

In the terminal asteroid defence problem, different interception positions have a great influence on the interception scheme, and it is necessary to select a suitable interception position. In this study, the interception position is expressed by the distance,  $d_p$ , of the interception position from the Earth, and it is assumed that the kinetic energy effect of the intercepting satellite on the asteroid is completed in one instant, that is, an impulse velocity increment,  $\Delta v$ , is applied to the asteroid. To keep the asteroid as far away from the Earth as possible, the direction of the impulse velocity increment is perpendicular to the asteroid velocity vector and coplanar with the asteroid orbital plane and pointing outward, as shown in Equation (7):

$$\frac{\Delta v}{\|\Delta v\|} = \frac{v_a \times (r_a \times v_a)}{\|v_a \times (r_a \times v_a)\|} \quad (7)$$

where  $\Delta v$  is the impulse velocity increment applied to the asteroid,  $v_a$  is the velocity vector of the asteroid, and  $r_a$  is the position vector of the asteroid.

To maintain the asteroid at a safe distance from the Earth, the magnitude of the impulse velocity increment applied to the asteroid at the intercept position is related to the asteroid intercept position and the safe distance. For an asteroid with a known position and velocity, the planned intercept position can be derived from orbital dynamics theory based on the planned intercept time. Therefore, the magnitude of the impulse velocity increment applied to the asteroid at the intercept position can be expressed as Equations (8) and (9):

$$d_p = g(t_p) \quad (8)$$

$$\|\Delta v\| = f_1(d_p, r_{\text{safe}}) = f_1(g(t_p), r_{\text{safe}}) = f_2(t_p, r_{\text{safe}}) \quad (9)$$

where  $d_p$  is the distance of the interception position from the Earth,  $r_{\text{safe}}$  is the safe distance from the Earth, and  $t_p$  is the planned intercept time.

**Remark 2.** It is worth mentioning that the essence of the analysis of the planned interception position and the planned interception time is the same because they are variables with a mapping relationship, not independent.

This section explores the mapping relationship between the planned intercept time and the magnitude of the impulse velocity increment acting on the target asteroid to guide task allocation and intercept orbit planning. For an asteroid with a close impact threat, let the time of discovery of the asteroid be  $t_0$  and the time of impact on the Earth without



active defence be  $t_{\text{end}}$ , so the interception time interval is  $(t_0, t_{\text{end}})$ . The analysis method of the asteroid interception position in this section is designed as follows.

- Step 1: Traverse the entire interception time interval  $(t_0, t_{\text{end}})$  with  $t_{\text{step}}$  as the time step to obtain  $n$  interception times,  $t_i = i \cdot t_{\text{step}}, i = 1, 2, \dots, n$  and  $n = (t_{\text{end}} - t_0)/t_{\text{step}}$ . Create a main loop  $i = 1, 2, \dots, n$ .
- Step 2: In the main loop, for each interception time  $t_i$ , the corresponding interception position  $d_p$ , asteroid position  $r_{a,i}$ , and velocity  $v_{a,i}$  are calculated by orbital dynamics theory based on the initial state of the asteroid.
- Step 3: Create a subloop, starting from  $j = 0$ . Apply an impulse manoeuvre  $\|\Delta v_j\| = j \cdot v_{\text{step}}$  to the asteroid with  $v_{\text{step}}$  as the step, obtaining the new asteroid velocity,  $v_{a,i'} = v_{a,i} + \Delta v_j$ , where the direction of  $\Delta v_j$  is determined by Equation (7).
- Step 4: Based on the asteroid position vector and the new velocity vector, calculate the asteroid orbit, and calculate the minimum distance to the Earth,  $d_{\text{min}}$ . If  $d_{\text{min}} > r_{\text{safe}}$ , the defence is successful, record the current  $\|\Delta v_j\|$ , which is the magnitude of the impulse velocity increment required for the defence, and the subloop ends, go to Step 2 to continue the main loop. If  $d_{\text{min}} \leq r_{\text{safe}}$ , then  $j = j + 1$  and return to Step 3 to continue the subloop.
- Step 5: Finally, after the end of the main cycle, for each interception time  $t_i$ , the corresponding  $\|\Delta v\| - t_p$  and  $\|\Delta v\| - d_p$  graphs are plotted.

Based on the number of available interceptor satellites,  $n$ , and the impulse,  $I_s$ , that can be provided by the asteroid impulse generator, the maximum total impulse velocity increment  $\|\Delta v_{\text{total}}\|$  that is provided by the available interceptor satellite formation can be calculated by Equation (10):

$$\|\Delta v_{\text{total}}\| = \frac{\|I_s\|}{m_0} \quad (10)$$

Therefore, the interception time,  $t_p$ , that satisfies  $\|\Delta v\| \leq \|\Delta v_{\text{total}}\|$  should be selected based on the plotted  $\|\Delta v\| - t_p$  function diagram.

**Remark 3.** This section analyses the effect of the planned interception time on the required impulse velocity increment to the asteroid. However, the merit of the asteroid interception scheme also needs to consider the manoeuvring capability required to intercept the satellite. The purpose of analysing the impact of interception time,  $t_p$ , is to support the defence task allocation. Specifically, (1) obtain the variation pattern of the required impulse velocity increment of the asteroid with the interception time  $t_p$ , and (2) when the interception time  $t_p$  is selected, the number of satellites required for interception can be derived from the results of the analysis in this section. The required number of interceptions is an indispensable parameter in the defence mission allocation.

#### 4. Defence Task Allocation Considering the Lambert Orbital Manoeuvre

In this section, after determining the interception position and interception time based on the analysis results of Section 3, the contract net protocol algorithm considering the Lambert orbital manoeuvre is proposed to realise defence task allocation and transfer orbit planning.

##### 4.1. Contract Net Protocol Algorithm Framework

The contract net protocol algorithm consists of three phases, which are the task announcement phase, the bidding phase, and the contract signing phase, as shown in Figure 4.

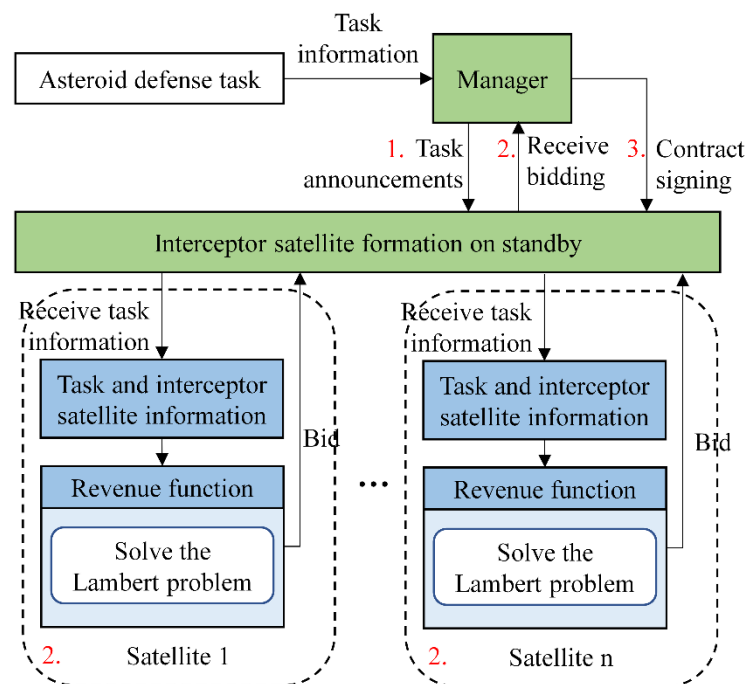


**Figure 4.** Schematic diagram of the improved contract net protocol algorithm.

(1) Task announcement phase.

Task information is released to the interceptor satellite formations, and each interceptor satellite obtains the specific details of the defence task.

(2) Bidding phase.

Each interceptor satellite constructs the task allocation revenue function based on the interception time of the task, the satellite’s own manoeuvring capability, orbital elements, and other information, and sends the revenue function to the manager. In this process, the construction and computation of the revenue function are critical in determining the performance of the task allocation algorithm. The revenue function in this study considers the orbit planning of intercepting satellites, and the specific revenue function form and calculation method will be presented in Section 4.2.

(3) Contract signing phase.

According to the revenue function of each interceptor satellite, the manager selects the winning interceptor satellite with the largest revenue function and updates the task allocation list. The whole process is cycled until all the tasks are assigned.

4.2. Revenue Function Construction for the Contract Net Protocol Algorithm

The result of the defence task allocation is one of the factors that affect the interceptor satellite orbital manoeuvre, and the satellite orbital manoeuvring strategy in turn affects the defence mission allocation. The traditional task allocation method only considers the attributes of performers, and the mission execution effect is different from reality. In this study, we consider the Lambert orbital manoeuvre in the contract net protocol algorithm and implement the orbital manoeuvre decision at the same time as the mission assignment by calculating the impulse velocity increment required for rendezvous. The performance of the task allocation algorithm is largely determined by the revenue function. The revenue function in this study is set as shown in Equation (11):

$$R = V_s - (||dv_{s1}|| + ||dv_{s2}||) \tag{11}$$

where  $V_s$  denotes the available total impulse velocity increment of the interceptor satellites,  $dv_{s1}$  denotes the required first impulse velocity increment for the interceptor satellite to



transfer manoeuvre, and  $dv_{s2}$  denotes the required second impulse velocity increment for the interceptor satellite to transfer manoeuvre.

If the required impulse velocity increment is greater than the available impulse velocity increment, the satellite is unable to complete the defence mission. If multiple satellites are able to complete the defence mission, the algorithm tends to select the satellite with less energy consumption to retain more energy for potential emergencies.

**Remark 4.** *The  $V_s$  term in the revenue function is a property of the satellite itself, while the  $\|dv_{s1}\|$  and  $\|dv_{s2}\|$  terms are related not only to the interceptor satellite itself but also to the transfer orbit. Therefore, the calculation of the revenue function for each interceptor satellite also requires solving the orbital manoeuvre problem for the interceptor satellite. For the double-impulse orbital manoeuvre, the Lambert problem can be solved to derive for each interceptor satellite the impulse velocity increment required to reach the planned intercept position at the planned interception moment.*

**Remark 5.** *To solve the  $\|dv_{s1}\|$  and  $\|dv_{s2}\|$  terms in the revenue function and to implement the orbit planning of satellites, the Lambert rendezvous problem needs to be solved. For a long-range double-impulse interception problem with a known interception time and a known interception position, obtaining its transfer orbit is a typical Lambert problem. Then, the required impulse velocity increment for the orbital manoeuvre of the intercepting satellite can be obtained.*

The Lambert problem can be described as follows. The starting position,  $r_1$ , the ending position,  $r_2$ , and the manoeuvre time,  $\Delta t = t_{\text{end}} - t_0$ , of the orbital manoeuvre are known, and the orbital elements of the satellite's transfer orbit are determined. Then, the satellite velocity vector,  $v_0$ , at moment  $t_0$  of the manoeuvre can be solved based on the orbital elements, and thus, the velocity impulse increment,  $\Delta v$ , applied to the satellite at that moment can be calculated. Since the Lagrange method of the two-body Lambert problem is very mature and well-known, it is not repeated here.

## 5. Simulations

### 5.1. Simulation Setup

The simulation experiments were performed in the Python environment on a desktop computer with an Intel(R) Core(TM) i7-10700 CPU at 2.90 GHz and 16 GB RAM. In the simulation experiment of this study, the central body was the Earth, and the minimum time step for the scenario was 600 s. Since most existing spacecraft run on and below the geosynchronous orbit, an altitude of 40,000 km was set as the safe distance,  $r_{\text{safe}}$ , herein. The on-orbit standby interceptor formation had 12 satellites. The available total impulse velocity increment of the interceptor satellites was  $V_s = 7$  km/s, and the impulse magnitude that the asteroid impulse generator can provide was  $I_s = 10^{11}$  (kg · m/s). In present technological terms, it is still difficult to realise it. The main difficulties are as follows: (1) the difficulty to provide a sufficiently large impulse, and (2) the difficulty to ensure the controlled direction of the impulse applied to the asteroid. However, recent technological developments allow serious consideration of such a defence scenario and method. The orbital elements of the interceptor satellites were set as shown in Table 1.

The initial position of the asteroid with an impact threat is located at the boundary of the Earth's gravitational capture range, and its position and velocity vector were set as in Table 2. The initial flight trajectory of the asteroid is shown in Figure 5.

According to the orbital dynamics propagation and the analysis of the above figure, it was known that the asteroid will hit the Earth at 195,000 s. Therefore, the asteroid setup in this study met the research requirements.

**Table 1.** The orbital elements of our interceptor satellites.

Orbital Elements	Symbol	Value	Unit	Remarks
Semi-major axis	$a$	38,000	km	$k = 1, 2, 3$ denotes the orbital plane serial number, $j = 1, 2, 3, 4$ denotes the satellite serial number within the orbital plane
Eccentricity	$e$	0	-	
Orbital inclination	$i$	53	deg	
Argument of periapsis	$\omega$	0	deg	
Right ascension of ascending node	$\Omega$	$k \cdot 120$	deg	
True anomaly	$\varphi$	$j \cdot 90 - 165$	deg	

**Table 2.** The position and velocity vector of the asteroid.

Asteroid State	Symbol	Value	Unit
Position vector	$r$	$[-68,662.408, 351,593.459, 34,040.410]$	km
Velocity vector	$v$	$[0.01951218, -1.09871708, -0.10637507]$	km/s
Mass	$m_0$	$10^9$	kg

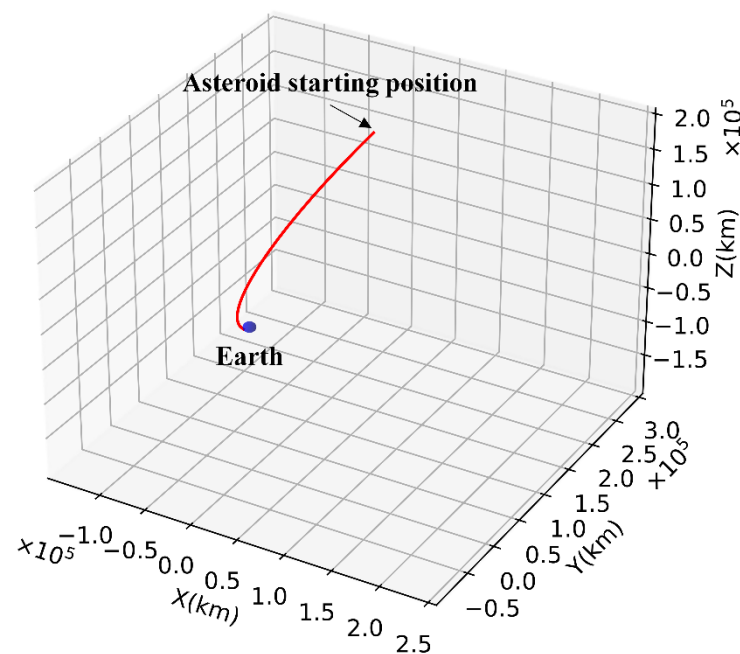


**Figure 5.** The initial flight trajectory of the asteroid.

5.2. Simulation Results

5.2.1. Analysis of Asteroid Interception Opportunity

The impact time of the asteroid was 195,000 s, and the time for the asteroid to enter the safe distance was 188,400 s. According to the time step of 600 s in this study, there were 314 optional interception times before entering the safe distance. In this study, 162 planned interception time points,  $t_i = 1200 \cdot i(s), i = 1, 2, \dots, 162$ , were obtained sequentially, with 1200 s as the time interval.

This section outlines that 78 simulations were performed to solve for the required impulse increments  $\|\Delta v\|$  applied to the asteroid for planned interception time  $t_i$ . The whole graph of  $\|\Delta v\| - t_i$  and  $\|\Delta v\| - d_p$  variation is shown in Figure 6a,b.

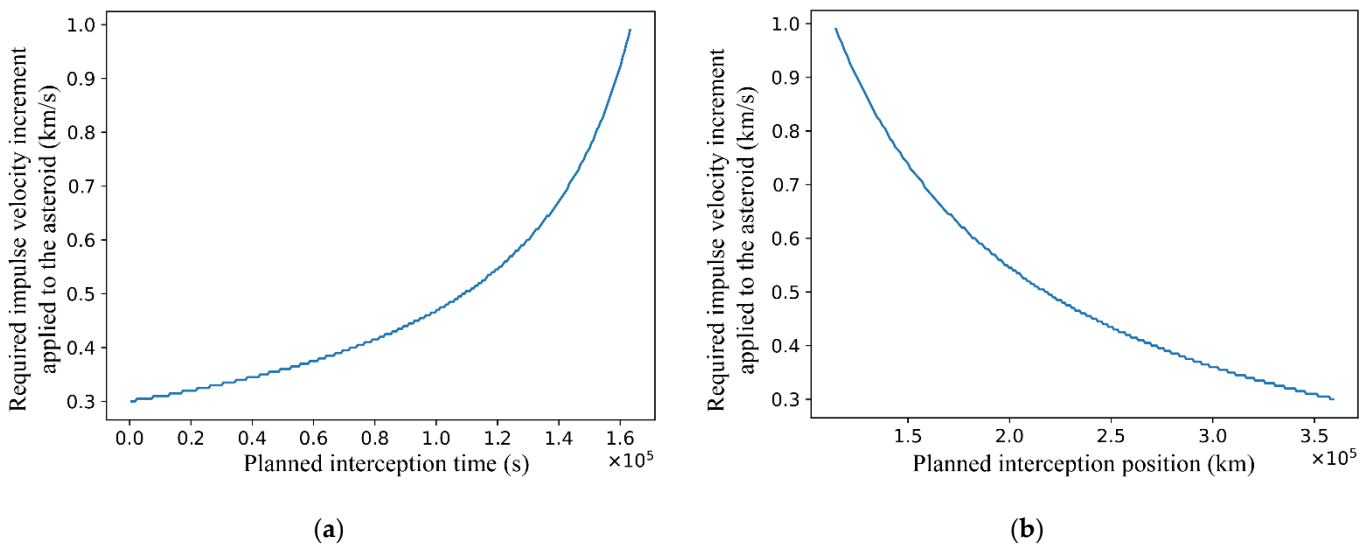


**Figure 6.** The graph of  $\|\Delta v\| - t_i$  and  $\|\Delta v\| - d_p$  variation. (a)  $\|\Delta v\| - t_i$  and (b)  $\|\Delta v\| - d_p$ .

In the above simulation experiment, when the planned interception time was greater than 163,200 s, the required impulse velocity increment applied to the asteroid was too large to be achieved and was therefore considered unsuccessful for defence. Within the range of successful defence, the earlier the planned interception time is, the further the planned interception position is from the Earth, and the smaller the required impulse velocity increment applied to the asteroid. However, the selection of the planned interception time also had to consider the impulse velocity increment required for interceptor satellite rendezvous. An earlier interception time will cause the intercepting satellite to consume more energy to reach the intercept position. When the planned interception time is too short, namely, when Equation (12) is satisfied, the interception missions will also fail.

$$\|dv_{s1}\| + \|dv_{s2}\| > V_s \tag{12}$$

Therefore, the choice of the planned interception time requires a combination of the required impulse velocity increment applied to the asteroid and the energy consumed by the interceptor satellite orbital manoeuvre.

Once an interception time,  $t_i$ , is selected, the number of interceptor satellites is known by referring to the graph of  $\|\Delta v\| - t_i$ . Thus, the asteroid defence mission assignment corresponding to that interception time,  $t_i$ , can be made.

### 5.2.2. Comparison Simulations of Asteroid Terminal Defence Using the Proposed Technique

According to Equation (10), the maximum impulse velocity increment that each interceptor satellite can provide is  $\|\Delta v_i\| = 0.1$  km/s. To ensure universality and representativeness,  $t_i = 60,000$  s,  $t_i = 120,000$  s, and  $t_i = 160,200$  s were selected as examples in this section. In these three cases, defence task allocation and interception trajectory planning were performed.

- (1) Defence task allocation and interception orbit planning when  $t_i = 60,000$  s.

When  $t_i = 60,000$  s, according to the analysis in Section 5.2.1, the required impulse velocity increment applied to asteroid  $\|\Delta v\|$  is 0.375 km/s. Therefore, referring to the graph of  $\|\Delta v\| - t_i$ , the defence task requires four interceptor satellites in coordination. The revenue function in the contract net protocol algorithm is shown in Figure 7. According to the revenue function diagram, no satellite has positive revenue functions; that is, no interceptor satellite can rendezvous with the asteroid. The planned interception time is too short, and although the impulse velocity increment required for the asteroid is small, the

impulse velocity increment required for the interceptor satellite rendezvous is too large to rendezvous with the asteroid. Therefore, the asteroid interception fails when  $t_i = 60,000$  s.

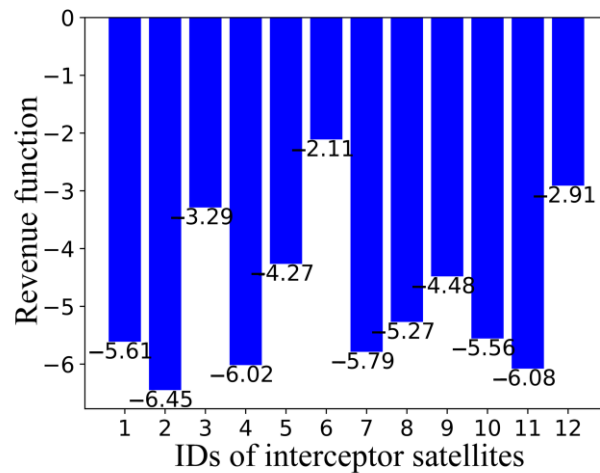


Figure 7. Revenue function when  $t_i = 60,000$  s.

(2) Defence task allocation and interception orbit planning when  $t_i = 120,000$  s.

When  $t_i = 120,000$  s, according to the analysis in Section 5.2.1, the required impulse velocity increment applied to asteroid  $\|\Delta v\|$  is 0.545 km/s. Therefore, referring to the graph of  $\|\Delta v\| - t_i$ , the defence task requires six interceptor satellites in coordination. The revenue function in the contract net protocol algorithm is shown in Figure 8a, and the total trajectory diagram of the asteroid and the intercepted satellites is shown in Figure 8b. The interceptor satellites assigned to the defence task were satellites No. 3, No. 5, No. 6, No. 8, No. 10, and No. 12. When  $t_i = 120,000$  s, the number of interceptor satellites required was moderate, and the impulse velocity increment required for interceptor satellite rendezvous was less than  $V_s$ .

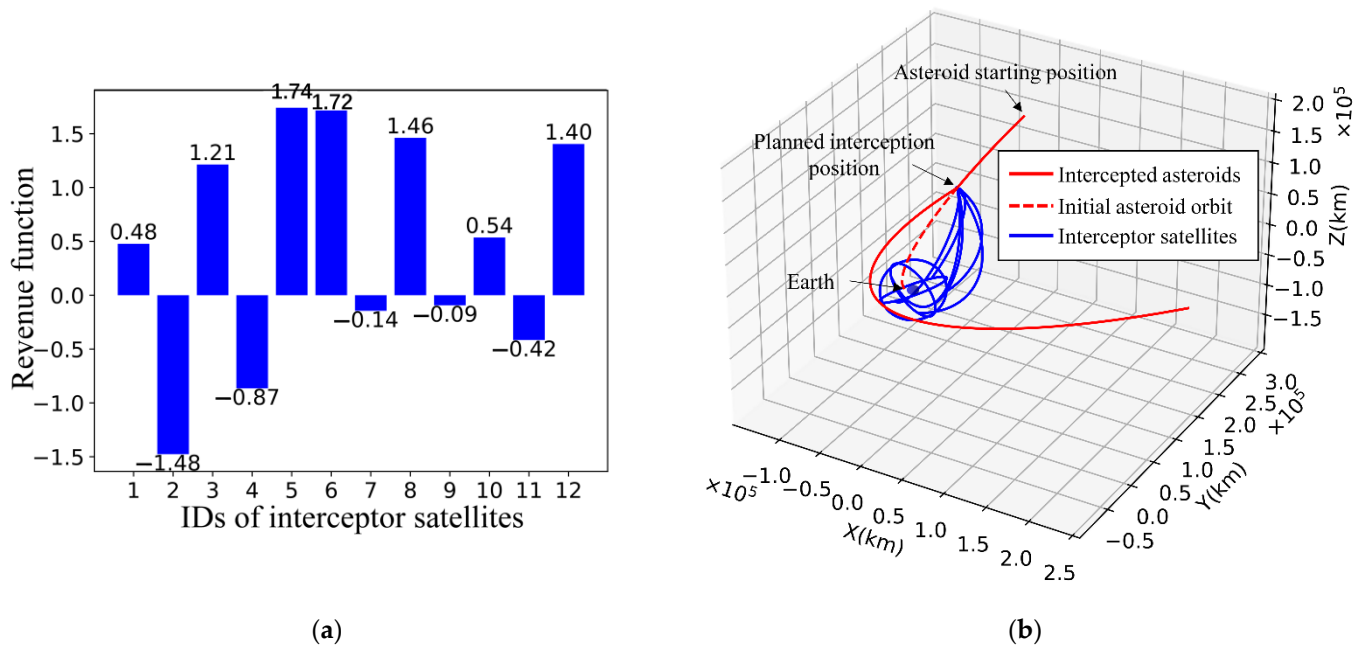


Figure 8. Simulation results when  $t_i = 120,000$  s. (a) Revenue function. (b) Total trajectory diagram.

(3) Defence task allocation and interception orbit planning when  $t_i = 160,200$  s.

When  $t_i = 160,200$  s, according to the analysis in Section 5.2.1, the required impulse velocity increment applied to asteroid  $\|\Delta v\|$  is 0.925 km/s. Therefore, referring to the

graph of  $\|\Delta v\| - t_i$ , the defence task requires 10 interceptor satellites in coordination. The revenue function in the contract net protocol algorithm is shown in Figure 9a, and the total trajectory diagram of the asteroid and the intercepted satellites is shown in Figure 9b. The interceptor satellites assigned to the defence task were No. 1, No. 3, No. 5, No. 6, No. 7, No. 8, No. 9, No. 10, No. 11, and No. 12 satellites. When  $t_i = 160,200$  s, the number of interceptor satellites required is higher, and the impulse velocity increment required for interceptor satellite rendezvous is less than  $V_s$ .

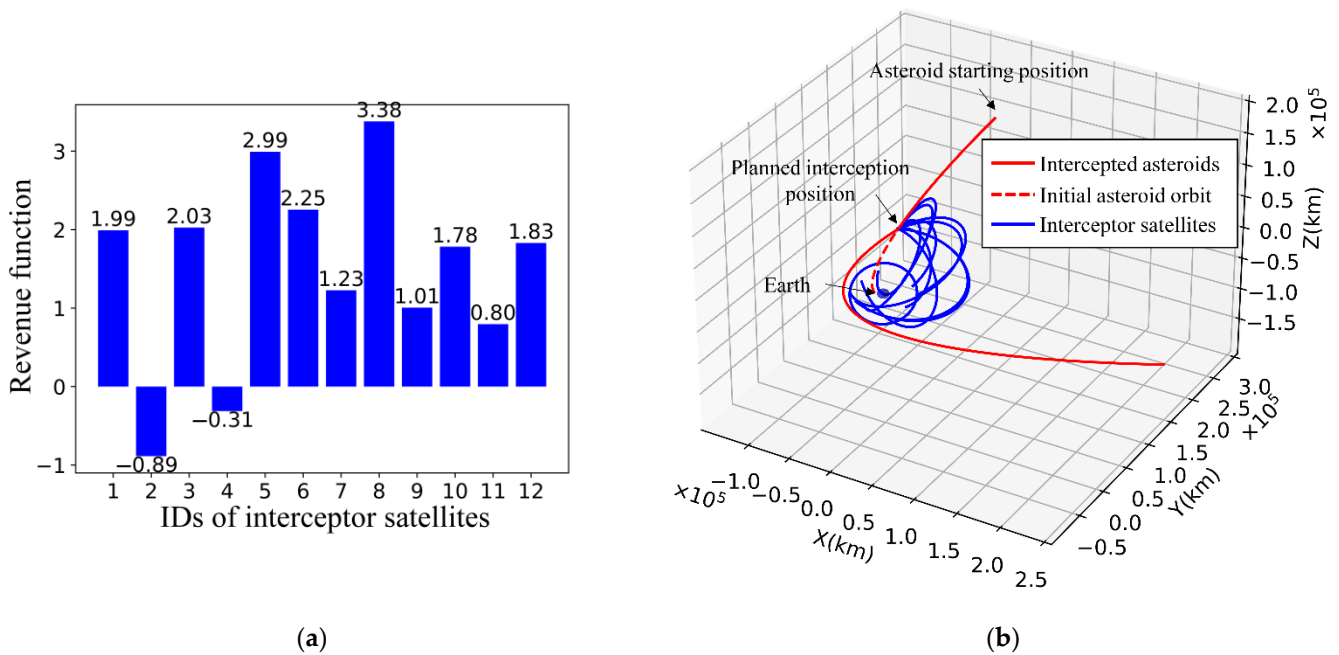


Figure 9. Simulation results when  $t_i = 160,200$  s. (a) Revenue function. (b) Total trajectory diagram.

5.2.3. Analysis and Discussion

The evaluation indices comparing the above three cases are shown in Figure 10. The analysis of the above three results showed that the earlier the planned interception time is, the further the interception position is from the Earth.

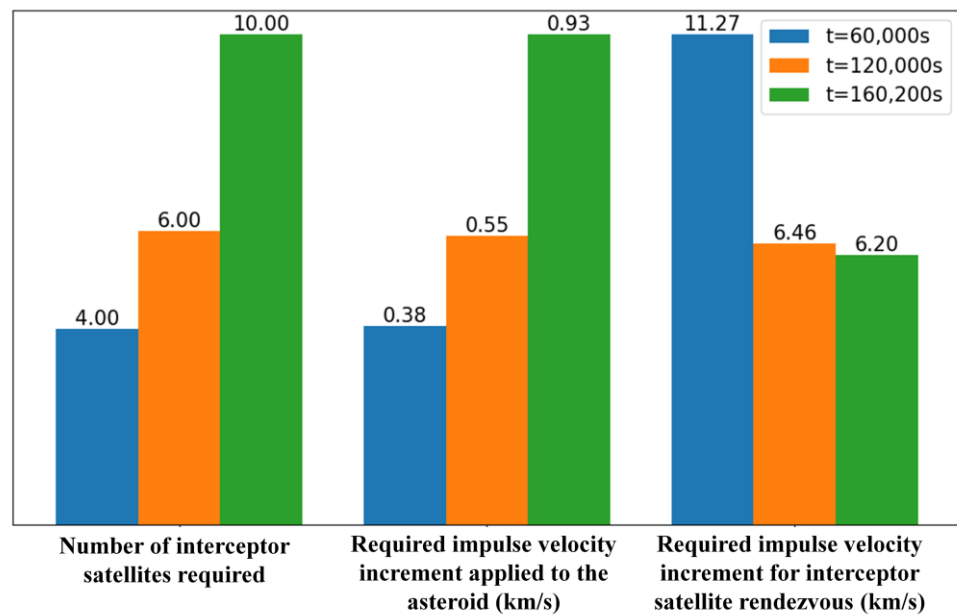


Figure 10. Comparison of evaluation indices.

Although the required impulse velocity increment applied to the asteroid is smaller, the required impulse velocity increment for the interception satellite orbital manoeuvre is larger. Among the above three cases, the case of  $t_i = 60,000$  s required the smallest impulse velocity increment applied to the asteroid, so the number of interceptor satellites required was the smallest. However, the impulse velocity increment required for the interceptor satellite to transfer manoeuvre was too large to be satisfied by current satellites. Therefore, the asteroid interception mission fails when  $t_i = 60,000$  s. The manoeuvring capabilities of the interceptor satellites met the rendezvous requirements in both the cases of  $t_i = 120,000$  s and  $t_i = 160,200$  s, but the number of required interceptor satellites was smaller in the cases of  $t_i = 120,000$  s. In a comprehensive comparison, the case of  $t_i = 120,000$  s was more appropriate, and the required impulse velocity increment applied to the asteroid and the impulse velocity increment required for the interceptor satellite to transfer manoeuvre both fell within the acceptable range.

## 6. Conclusions

An asteroid defence method based on multisatellite interception was presented in this study. Through the assessment of asteroid interception position selection, the influence law of the interception position on the required impulse velocity increment applied to the asteroid was revealed. The closer the planned interception position is to the Earth, the larger the required impulse velocity increment applied to deflect the orbit of the asteroid. This law can be the basis and rule for interception opportunity selection, task allocation, and orbit planning. By taking the intercepting satellite orbit manoeuvre as one part of the revenue function, the improved contract net protocol algorithm coupled with the Lambert orbital manoeuvre can provide effective task allocation and intercept orbits for multiple on-orbit satellites to fulfil asteroid terminal defence. In this manner, the asteroid orbit can be deflected a safe distance from the Earth. Simulation experiments demonstrate that rationally allocated multisatellite interception is an effective means for terminal defence of the invading asteroid within the sphere of the gravitational influence of the Earth.

**Author Contributions:** Conceptualisation, X.J. and Y.L.; methodology, X.J. and Y.L.; software, Y.L.; validation, X.J. and Y.L.; formal analysis, X.J. and Y.L.; investigation, X.J., Y.L., S.Z., Y.J. and G.S.; resources X.J., S.Z. and Y.J.; data curation, X.J. and Y.L.; writing—original draft preparation, Y.L.; writing—review and editing, X.J.; visualisation, Y.L.; supervision, X.J.; project administration, X.J.; funding acquisition, X.J. All authors have read and agreed to the published version of the manuscript.

**Funding:** This work is supported by Open Funding of the National Defense Science and Technology Key Laboratory of Space Intelligent Control Technology (Grant No. 6142208200304), the Qian Xuesen Laboratory of Space Technology, CAST (Grant No. GZZKFJJ2020001), and the Postdoctoral Research Foundation of Sichuan University.

**Institutional Review Board Statement:** Not applicable.

**Informed Consent Statement:** Informed consent was obtained from all subjects involved in the study.

**Data Availability Statement:** Not applicable.

**Acknowledgments:** The authors fully appreciate the funders' financial supports.

**Conflicts of Interest:** The authors declare no conflict of interest.

## References

1. Wu, W.R.; Gong, Z.Z.; Tang, Y.H.; Zhang, P.L. Response to risk of near-earth asteroid impact. *Strateg. Study CAE* **2022**, *24*, 140–151. [[CrossRef](#)]
2. Silber, E.A.; Boslough, M.; Hocking, W.K.; Gritsevich, M.; Whitaker, R.W. Physics of meteor generated shock waves in the Earth's atmosphere—A review. *Adv. Space Res.* **2018**, *62*, 489–532. [[CrossRef](#)]
3. Chyba, C.F.; Thomas, P.J.; Zahnle, K.J. The 1908 Tunguska explosion: Atmospheric disruption of a stony asteroid. *Nature* **1993**, *361*, 40–44. [[CrossRef](#)]



4. Brown, P.G.; Assink, J.D.; Astiz, L.; Blaauw, R.; Boslough, M.B.; Borovička, J.; Brachet, N.; Brown, D.; Campbell-Brown, M.; Ceranna, L.; et al. A 500-kiloton airburst over Chelyabinsk and an enhanced hazard from small impactors. *Nature* **2013**, *503*, 238–241. [[CrossRef](#)]
5. Galimov, E.M.; Kolotov, V.P.; Nazarov, M.A.; Kostitsyn, Y.A.; Kubrakova, I.V.; Kononkova, N.N.; Roshchina, I.A.; Alexeev, V.A.; Kashkarov, L.L.; Badyukov, D.D.; et al. Analytical results for the material of the Chelyabinsk meteorite. *Geochem. Int.* **2013**, *51*, 522–539. [[CrossRef](#)]
6. Martino, S.; Tancredi, G.; Monteiro, F.; Lazzaro, D.; Rodrigues, T. Monitoring of asteroids in cometary orbits and active asteroids. *Planet. Space Sci.* **2019**, *166*, 135–148. [[CrossRef](#)]
7. Wang, Y.; Xu, S.J. Non-equatorial equilibrium points around an asteroid with gravitational orbit-attitude coupling perturbation. *Astrodynamics* **2020**, *4*, 1–16. [[CrossRef](#)]
8. Li, X.Y.; Qiao, D.; Barucci, M.A. Analysis of equilibria in the doubly synchronous binary asteroid systems concerned with non-spherical shape. *Astrodynamics* **2018**, *2*, 133–146. [[CrossRef](#)]
9. Wei, B.W.; Shang, H.B.; Qiao, D. Hybrid model of gravitational fields around small bodies for efficient trajectory propagation. *J. Guid. Control. Dyn.* **2020**, *43*, 232–249. [[CrossRef](#)]
10. Zhang, Y.; Yu, Y.; Baoyin, H.X. Dynamical behavior of flexible net spacecraft for landing on asteroid. *Astrodynamics* **2021**, *5*, 249–261. [[CrossRef](#)]
11. Liu, X.W.; Yang, H.W.; Li, S. Collision-free trajectory design for long-distance hopping transfer on asteroid surface using convex optimization. *IEEE Trans. Aerosp. Electron. Syst.* **2021**, *57*, 3071–3083. [[CrossRef](#)]
12. Hao, Z.W.; Zhao, Y.; Chen, Y.; Zhang, Q.H. Orbital maneuver strategy design based on piecewise linear optimization for spacecraft soft landing on irregular asteroids. *Chin. J. Aeronaut.* **2020**, *33*, 2694–2706. [[CrossRef](#)]
13. Yang, H.W.; Bai, X.L.; Baoyin, H.X. Rapid generation of time-optimal trajectories for asteroid landing via convex optimization. *J. Guid. Control. Dyn.* **2017**, *40*, 628–641. [[CrossRef](#)]
14. Yang, H.W.; Li, S.; Bai, X.L. Fast homotopy method for asteroid landing trajectory optimization using approximate initial costates. *J. Guid. Control. Dyn.* **2019**, *42*, 585–597. [[CrossRef](#)]
15. Schirru, L.; Pisanu, T.; Podda, A. The ad hoc back-end of the BIRALET radar to measure slant-range and Doppler shift of resident space objects. *Electronics* **2021**, *10*, 577. [[CrossRef](#)]
16. Ionescu, L.; Rusu-Casandra, A.; Bira, C.; Tatomirescu, A.; Tramandan, I.; Scagnoli, R.; Istrateanu, D.; Popa, A.E. Development of the Romanian radar sensor for space surveillance and tracking activities. *Sensors* **2022**, *22*, 3546. [[CrossRef](#)]
17. Ender, J.; Leushacke, L.; Brenner, L.; Wilden, H. Radar Techniques for Space Situational Awareness. In Proceedings of the IEEE International Radar Symposium (IRS), Leipzig, Germany, 7–9 September 2011.
18. European Space Surveillance and Tracking Program. Available online: <https://www.eusst.eu/> (accessed on 30 June 2022).
19. Yu, Z.T.; Shang, H.B.; Wei, B.W. Accessibility assessment and trajectory design for multiple Near-Earth-asteroids exploration using stand-alone CubeSats. *Aerosp. Sci. Technol.* **2021**, *118*, 106944. [[CrossRef](#)]
20. Cheng, A.F.; Atchison, J.; Kantsiper, B.; Rivkin, A.S.; Stickle, A.; Reed, C.; Galvez, A.; Carnelli, I.; Michel, P.; Ulamecd, S. Asteroid impact and deflection assessment mission. *Acta Astronaut.* **2015**, *115*, 262–269. [[CrossRef](#)]
21. Wagner, S.; Wie, B.; Barbee, B.W. Target selection for a hypervelocity asteroid intercept vehicle flight validation mission. *Acta Astronaut.* **2015**, *107*, 247–261. [[CrossRef](#)]
22. Wie, B.; Zimmerman, B.; Lyzhoft, J.; Vardaxia, G. Planetary defense mission concepts for disrupting/pulverizing hazardous asteroids with short warning time. *Astrodynamics* **2017**, *1*, 3–21. [[CrossRef](#)]
23. Lubin, P.; Hughes, G.B.; Eskenazi, M.; Kosmo, K.; Johansson, I.S.; Griswold, J.; Pryor, M.; O'Neill, H.; Meinhold, P.; Suen, J.; et al. Directed energy missions for planetary defense. *Adv. Space Res.* **2016**, *58*, 1093–1116. [[CrossRef](#)]
24. Tsuda, Y.; Takeuchi, H.; Ogawa, N.; One, G.; Kikuchi, S.; Oki, Y.; Ishiguro, M.; Kuroda, D.; Urakawa, S.; Okumura, S.; et al. Rendezvous to asteroid with highly uncertain ephemeris: Hayabusa2's Ryugu-approach operation result. *Astrodynamics* **2020**, *4*, 137–147. [[CrossRef](#)]
25. Yue, Y.X.; Shan, H.L.; Zhou, Z.W.; Wang, X.H. A fast calculation method for asteroid exploration window based on optimal and sub-optimal two-impulse transfer orbits. *Acta Astronaut.* **2021**, *186*, 171–182. [[CrossRef](#)]
26. Mathias, D.L.; Wheeler, L.F.; Dotson, J.L. A probabilistic asteroid impact risk model: Assessment of sub-300 m impacts. *Icarus* **2017**, *289*, 106–119. [[CrossRef](#)]
27. Zhang, F.; Xu, B.; Circi, C.; Zhang, L. Rotational and translational considerations in kinetic impact deflection of potentially hazardous asteroids. *Adv. Space Res.* **2017**, *59*, 1921–1935. [[CrossRef](#)]
28. Peak, S.W.; Weck, O.; Hoffman, J.; Binzel, R.; Miller, D. Optimization and decision-making framework for multi-staged asteroid deflection campaigns under epistemic uncertainties. *Acta Astronaut.* **2020**, *167*, 23–41. [[CrossRef](#)]
29. Sankaran, K.; Griffith, S.A.; Thompson, N.C.; Lochridge, M.D.; O'Kins, A.S. A parallelized genetic algorithm to evaluate asteroid impact missions using electric propulsion. *Aerospace* **2022**, *9*, 116. [[CrossRef](#)]
30. Kim, G.; Jeon, S.; Kee, C.; No, T.S.; Kwon, K.; Choi, S. GPS satellite state vector determination in ECI coordinate system using the civil navigation message. *J. Navig.* **2014**, *67*, 1–16. [[CrossRef](#)]
31. Yang, B.; Liu, P.X.; Feng, J.L.; Li, S. Two-stage pursuit strategy for incomplete-information impulsive space pursuit-evasion mission using reinforcement learning. *Aerospace* **2021**, *8*, 299. [[CrossRef](#)]